BIOLOGY OF REPRODUCTION **62,** 1745–1753 (2000)

Involvement of Mitochondria in Oxidative Stress-Induced Cell Death in Mouse Zygotes[1]

Lin Liu,[3,4] James R. Trimarchi,[3,4] and David L. Keefe[2,3,4]

Department of Obstetrics & Gynaecology,[3] Women & Infants Hospital, Brown University, Providence, Rhode Island 02905
Marine Biological Laboratory,[4] Woods Hole, Massachusetts 02543

ABSTRACT

Accumulation of reactive oxygen species during aging leads to programmed cell death (PCD) in many cell types but has not been explored in mammalian fertilized eggs, in which mitochondria are "immature," in contrast to "mature" mitochondria in somatic cells. We characterized PCD in mouse zygotes induced by either intensive (1 mM for 1.5 h) or mild (200 μM for 15 min) hydrogen peroxide (H_2O_2) treatment. Shortly after intensive treatment, zygotes displayed PCD, typified by cell shrinkage, cytochrome c release from mitochondria, and caspase activation, then terminal deoxynucleotidyl transferase-mediated dUTP nick end labeling (TUNEL) staining in condensed pronuclei. On the other hand, after mild treatment, zygotes arrested developmentally and showed neither cytochrome c release nor caspase activation over 48 h; until 72 h, 46% zygotes exhibited TUNEL staining, and 88% of zygotes lost plasma membrane integrity. Interestingly, mild oxidative treatment induced a decline in mitochondrial membrane potential and disruption of the mitochondrial matrix. Taken together, these results suggest that oxidative stress caused by H_2O_2 induces PCD in mouse zygotes and that mitochondria are involved in the early phase of oxidative stress-induced PCD. Furthermore, mitochondrial malfunction also may contribute to cell cycle arrest, followed by cell death, triggered by mild oxidative stress.

INTRODUCTION

Oxidative stress and mitochondrial decay are likely to be major contributors to aging and aging-associated cell death [1–7]. Hydrogen peroxide (H_2O_2), a form of reactive oxygen species (ROS), mediates mitochondrial oxidative damage that may lead to mitochondrial dysfunction and ultimately cell death, particularly when the mitochondrial antioxidant defense mechanisms are compromised, such as occurs during aging [8–11]. Alterations in mitochondrial structure and function have been shown to occur early during programmed cell death (PCD) or apoptosis, and mitochondria appear to be central regulators of apoptosis [12–15].

Oxidative stress, depending on its severity, can lead to either cell necrosis or apoptosis [16]. Necrosis is typified by cell and organelle swelling and leakage of intracellular contents into the extracellular milieu, resulting in inflammatory reaction. In contrast, apoptosis is characterized by cell shrinkage, membrane blebbing, and chromatin condensation [17–19]. However, the same inducer can cause either apoptosis or necrosis, depending on dose and duration [20]. Furthermore, secondary necrosis may occur during late stages of PCD [21] and may simply reflect an insufficient removal of apoptotic cells by phagocytes or neighboring cells [17]. Analyzing PCD in zygotes has advantages over other somatic cell systems in that zygotes are individual cells, and therefore confounding signaling from neighboring cells is absent. Moreover, effects of apoptotic signaling on subsequent development can be monitored in vitro.

Mitochondria mediate both apoptosis and necrotic forms of cell death [22]. The role of mitochondria in apoptosis of eggs is of interest because mitochondrial structure in eggs differs from that of somatic cell types. In eggs, mitochondria are electron-dense, with no obvious cristae from inner membrane [23], and therefore have been called immature. Zygotes can simply utilize pyruvate for energy production and produce limited ATP [24, 25]. It is unknown whether the immature mitochondria in oocytes or zygotes function differently during cell death, compared to mature mitochondria in most somatic cells.

Understanding PCD in mammalian embryos also may have clinical implications. Age-related decline in female fertility is a common phenomenon in older women and other long-lived mammals [26]. Maternal age has been demonstrated to affect oocyte quality and early embryonic development [27, 28]. During development, apoptotic cell death mediates follicular atresia and oocyte degeneration [29, 30]. Recently, it was found that PCD occurs in embryos that fail to execute essential developmental events during the first cell cycle [31]. In addition, both Bcl-2 (apoptotic inhibitor) and Bax (proapoptotic molecule) mRNA are present in preimplantation embryos [18, 32]. H_2O_2 has been shown to mediate PCD in the blastocyst [33], and fragmented human embryos contain high levels of H_2O_2 and exhibit evidence of PCD [34]. Elevated H_2O_2 levels also may be associated with the "2-cell block" that occurs in some mouse strains [35]. While there are no laboratory animal models for naturally occurring PCD during normal early embryo development, pharmacological models of mild oxidative stress might be an alternative way to mimic the chronic low levels of oxidative stress associated with aging.

The present studies first tested the hypothesis that mild or intensive oxidation caused by H_2O_2 induces PCD in mammalian zygotes. As mild oxidative stress more closely mimics chronic accumulative oxidative stress that occurs during aging [36], we further examined changes in mitochondrial structure and function after exposure to mild oxidation treatment.

[1]This work was supported in part by the National Institute of Health (NIH K081099) and Women and Infants Hospital/Brown Faculty Research Fund.
[2]Correspondence: David Keefe, Dept. of Ob-Gyn, Women & Infants Hospital, Brown University, 101 Dudley Street, Providence, RI 02905. FAX: 401 453 7599; e-mail: dkeefe@smtp.wihri.org

Received: 27 October 1999.
First decision: 24 November 1999.
Accepted: 27 January 2000.

ISSN: 0006-3363. http://www.biolreprod.org

MATERIALS AND METHODS

Reagents, Animals, Embryo Collection, and Culture

All reagents were purchased from Sigma Chemical Co. (St. Louis, MO), unless stated otherwise. Equine CG, used for superovulation, was purchased from Calbiochem (La Jolla, CA). B6C3F1 female mice, 6 wk old, were purchased from Charles River Laboratories (Boston, MA) and subjected to a 14L:10D light cycle for at least 1 wk before use. Animals were cared for according to procedures approved by the Marine Biological Laboratory and Women and Infants Hospital Animal Care Committees. Female mice were superovulated by i.p. injection of 7.5 IU eCG, followed 46–48 later by injection of 7.5 IU hCG, and then mated individually with B6C3F1 males with proven fertility. Next morning, females with vaginal plugs were selected and killed by cervical dislocation at 21–22 h after hCG injection. Zygotes (Day 1) enclosed in cumulus masses were released from the ampullae into KSOM (potassium simplex optimized medium) [37], buffered with 14 mM Hepes and 4 mM sodium bicarbonate, containing 0.03% hyaluronidase; then cumulus cells were removed by gentle pipetting [38]. Cumulus-free zygotes were washed and cultured in the KSOM supplemented with nonessential amino acids and 2.5 mM Hepes [37–39]. Embryos were cultured in 50-μl droplets of KSOM under mineral oil at 37°C in a humidified atmosphere of 7% CO_2 in air. H_2O_2 were appropriately diluted in KSOM for treatment of zygotes. Embryos were pooled and randomly distributed to each treatment group. Embryos were assessed for cleavage at Day 2 and then development to blastocysts at Day 4. Based on dose-response experiments, appropriate concentrations of H_2O_2 were chosen for further analysis in cell death experiments.

Live and Dead Assay

For cell death assessment, both the cell-impermeant dye propidium iodide (PI) and the cell-permeant dye Hoechst and fluorescence microscopy were employed [40, 41]. Embryos were stained with 20 μg/ml PI (Molecular Probes, Eugene, OR) and the cell-permeant dye Hoechst 33342 (20 μg/ml) for 15 min, washed, and then observed under an inverted microscope (Zeiss Axiovert 100TV, Oberkochen, Germany) equipped with fluorescence optics. Viable zygotes displayed a normal nuclear size and blue fluorescence in pronuclei under UV illumination. Dead zygotes manifested PI-positive stain (red) in pronuclei and brighter blue fluorescence in the cytoplasm. In addition, blebs of plasma membrane, shrinkage of cells, and condensation or fragmentation of nuclei also were considered indicative of apoptosis [18]. These morphological changes still provide the most reliable criteria for recognizing apoptosis [19].

Alternatively, the live/dead viability/cytotoxicity kit (Molecular Probes) [42] was used to detect live and dead embryos. Embryos were incubated with 2 μM calcein AM and 4 μM ethidium homodimer solution at 37°C for 20 min. Fluorescence was detected using a Zeiss Axiovert 100TV inverted fluorescence microscope. Live embryos displayed intense uniform green fluorescence (fluorescein filter), whereas dead embryos showed no green fluorescence but rather bright red fluorescence (rhodamine filter) (see Fig. 1). The results obtained from this live/dead kit were consistent with those obtained with the PI and Hoechst stains.

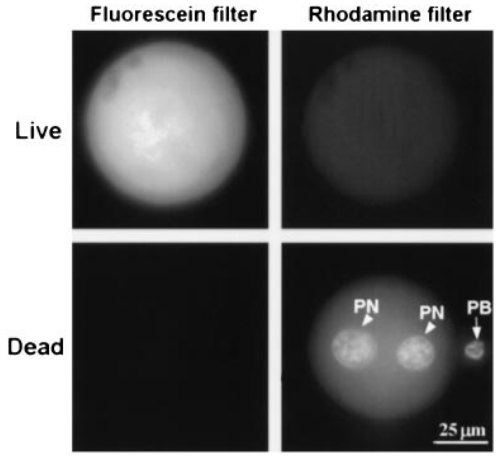

FIG. 1. Live and dead detection of cell death using the live/dead kit. Live zygotes exhibited green fluorescence throughout the cytoplasm under the fluorescein filter. Dead zygotes showed no cytoplasmic green fluorescence but strong red fluorescence, especially in the pronuclei. PN, Pronucleus; PB, polar body.

Detection of Apoptosis by Terminal Deoxynucleotidyl Transferase-Mediated dUTP Nick End-Labeling (TUNEL) Technique

Embryos were fixed in 3.7% paraformaldehyde in Dulbecco's PBS containing 0.1% polyvinylpyrrolidone (PVP). Nuclear DNA fragmentation in embryos was detected by the TUNEL method using the in situ cell death detection kit (Boehringer-Mannheim, Indianapolis, IN) and nuclei were counterstained with PI (50 μg/ml; Molecular Probes), as described previously [43, 44]. Fluorescence was detected using a Zeiss LSM 510 laser scanning confocal microscope or Zeiss Axiovert 100TV inverted fluorescence microscope.

Immunocytochemistry for Localization of Cytochrome c

Release of cytochrome c from mitochondria was assessed by immunocytochemistry [44–46], with some minor modifications made for assessment in mouse embryos. Briefly, embryos were fixed overnight at 4°C in 4% paraformaldehyde and permeabilized in 0.3% Triton X-100 for 30 min at room temperature. After being washed, embryos were blocked with PBS-PVP, supplemented with 5% normal goat serum for 45 min, then incubated with a mouse monoclonal anti-cytochrome c antibody (PharMingen, San Diego, CA) diluted at 1:50 in PBS-PVP supplemented with 5% normal goat serum for 2 h at room temperature. Embryos were washed extensively with PBS-PVP, then incubated with Texas Red anti-mouse IgG secondary antibody (Vector Laboratories, Burlingame, CA) diluted 1:100 for 45 min. Nuclei were stained with Hoechst 33258 (20 μg/ml) for 15 min. Embryos were mounted on a glass slide in Vectashield mounting medium (H-1000, Vector) and sealed. Cytochrome c localization was detected by fluorescence microscopy using Texas Red filter (excitation 595 nm, emission 610–615 nm) and UV filter for nuclear stain.

Caspase Activation Assay

Embryos were fixed in 4% paraformaldehyde overnight at 4°C, then blocked for 30 min in blocking serum solution (PBS-PVP supplemented with 5% normal goat serum and 0.3% Triton X-100). Afterward, embryos were incubated with a polyclonal rabbit anti-active caspase-3 antibody (PharMingen) diluted at 1:100 in blocking serum solution

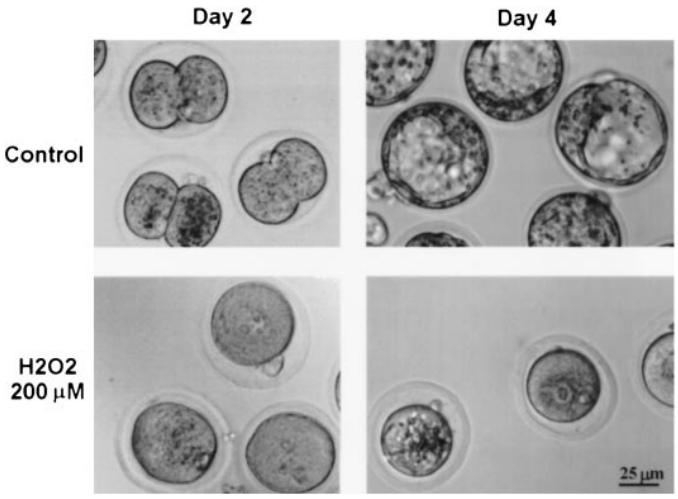

FIG. 2. Effects of H_2O_2 on development of mouse zygotes collected at Day 1. In untreated control culture, an average of 95% zygotes (n = 95) cleaved at Day 2, and 92% developed to blastocysts. Treatment of zygotes (n = 90) with 200 μM H_2O_2 inhibited cleavage and development, causing morphological hallmarks of apoptotic cell death, including cell shrinkage and membrane blebbing or cytoplasmic vacuoles.

overnight at 4°C. Embryos were washed thoroughly and then incubated in ABC solution with Vectastain Elit ABC Kit (Vector). Samples were reacted with diaminobenzidine solution until the desired brown intensity was obtained. The embryos were mounted on a slide and viewed with a transmitted light microscope.

Detection of Mitochondrial Membrane Potential (MMP) and Distribution of Active Mitochondria

MMP was measured with the lipophilic, cationic probe 5,5′,6,6′-tetrachloro-1,1′3,3′-tetraethylbenzimidazolylcarbocyanine iodide (JC-1; Molecular Probes) as described in previous reports [47, 48]. In the presence of a high MMP, JC-1 forms J-aggregates that emit red fluorescence, while JC-1 monomeric form emits green fluorescence at low MMP. Both colors were detected using a confocal microscope (Zeiss LSM510) with excitation at 488 nm and beam path control setting at LP 585 nm for Ch1 and BP 505–530 nm for Ch2. Embryos were incubated in 100 μl Hepes-buffered KSOM containing 1.25 μM JC-1 for 20 min at 37°C. Ratio analysis was performed with Zeiss LSM510 software and MetaMorph imaging software (UIC, Boston, MA).

The distribution of active mitochondria within cytoplasm was determined by rhodamine 123 (Rh123) [38, 49] or MitoTracker Red (personal communications with B.D. Bavister's laboratory, University of Wisconsin, Madison). Zygotes were incubated with either 10 μg/ml Rh123 or 330 nM MitoTracker Red (Molecular Probes) for 15 min, washed, and then observed with the same Zeiss fluorescence microscope as described above. Rh123 and MitoTracker showed the same staining pattern of active mitochondrial distribution, but the red fluorescence stained with MitoTracker lasted longer.

Transmission Electronic Microscopy

Embryos were fixed in 2.5% glutaraldehyde in 0.1 M phosphate buffer at 4°C for 1 h, washed in 0.1 M phosphate buffer, and embedded in agar chips. Subsequently, they were postfixed in 1% osmium tetroxide in 0.1 M phosphate buffer, pH 7.2; they were dehydrated and then embedded in Araldite/Epon (Electron Microscopy Sciences, Ft. Washington, PA) and sectioned into semithin sections, which were stained with toluidine blue. Then ultrathin sections were produced. The ultrathin sections were contrasted with uranyl acetate and lead citrate and then observed on a Zeiss 10CA transmission electron microscope.

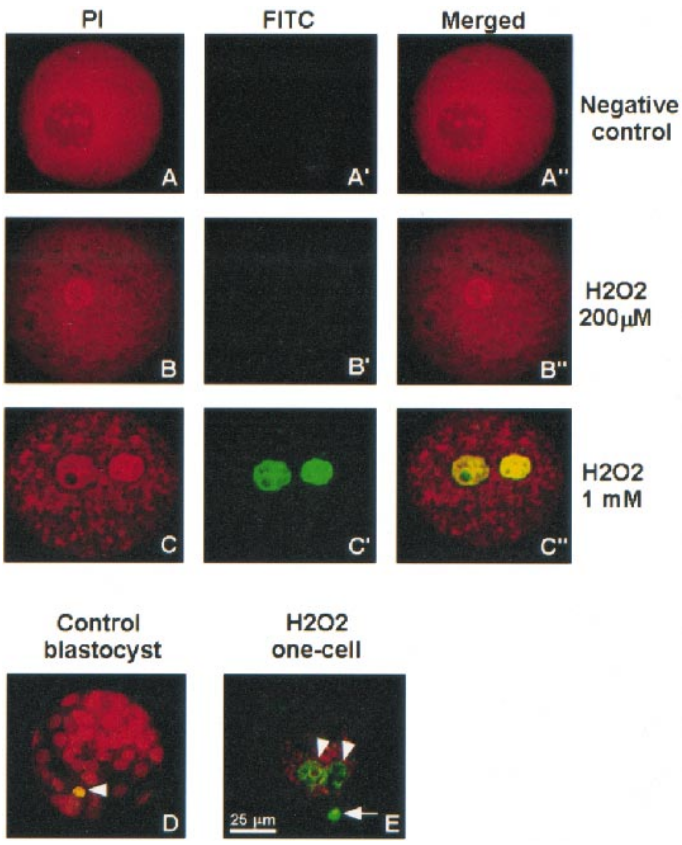

FIG. 3. TUNEL stain of cell death in mouse zygotes. In the negative control, the enzyme terminal deoxynucleotidyl transferase was not added. Top panels show negative control without enzyme added (**A**), TUNEL-negative stain in 200 μM H_2O_2-treated (15 min) zygotes (**B**), but positive stain (green fluorescence with fluorescein isothiocyanate filter) in 1 mM H_2O_2-treated (1.5 h) zygotes (**C**) within 24 h after treatment. Lower panels: TUNEL stain at Day 4 in a developed blastocyst as in control group (**D**) and 200 μM H_2O_2-arrested one-cell (**E**). Arrowhead indicates positive TUNEL nuclei, and arrow indicates polar body.

Statistical Analysis

Each treatment in the experiment was repeated at least twice. One-way ANOVA was utilized for comparisons of treatment means, such as cell number. The chi-square test was used for analysis of differences in the case of percentage comparison, such as rate of development. Significant difference was defined as $P < 0.05$, and no difference was defined as $P > 0.05$.

RESULTS

H_2O_2-Induced Zygotic Cell Death Characterized by Morphology and TUNEL Stain

In control culture, B6C3F1 mouse zygotes cleaved normally (95%) at Day 2 and developed to blastocysts (92%) by Day 4 (Fig. 2). In developed blastocysts, an average of 2 apoptotic cells were observed by TUNEL stain (Fig. 3D), a result similar to that shown previously [43]. As it has

TABLE 1. H_2O_2-Induced cell death in mouse zygotes.

Treatment	Hours after treatment	% Dead[a] (no. examined)	% TUNEL-positive[b] (no. examined)
Control	5	0 (50)	0 (30)
H_2O_2 (1 mM)	5–24	96 (67)	89 (37)
H_2O_2 (200 μM)[c]	24	0 (88)	0 (33)
	48	31 (83)	0 (24)
	72	88 (48)	46 (22)

[a] Live and dead stain includes both PI and Hoechst stain, and Live and Dead Kit; pooled data from at least 4 replicates.
[b] Pooled data from 3 replicates.
[c] Prior to 24 h after treatment, all zygotes were PI negative and did not exhibit TUNEL-positive staining (data not shown in this table); polar bodies showed FITC positive at 24–48 h (37%, n = 27) and 72 h (100%, n = 22).

been recognized that blastocysts exhibit PCD [32, 33, 43, 50], TUNEL-positive staining from blastocysts treated with H_2O_2 for 1 h were used as a positive control to confirm the effectiveness of this apoptotic assay applied in zygotes. Twenty-four hours after treatments, the total cell number (55 ± 19) was significantly ($P < 0.05$) reduced and percentage (25 ± 34%) of apoptotic cells significantly increased in blastocysts (n = 11) treated with 200 μM H_2O_2, compared to values for control, untreated blastocysts (106 ± 14 and 2 ± 2%, respectively, n = 14). However, 100 μM H_2O_2 treatment did not affect total as well as apoptotic cells in the blastocysts (112 ± 23 and 2 ± 3%, respectively, n = 11). In preliminary experiments, the effects of H_2O_2 on cleavage and development of zygotes or two-cell mouse embryos showed concentration and time dependence (data not shown).

Mild treatment of zygotes with 200 μM H_2O_2 for 15 min completely inhibited cleavage, and zygotes arrested at the one-cell stage thereafter (Fig. 2). Treated zygotes exhibited shrunken morphology, but failed to display PI-positive staining 24 h after treatment, when pronuclei were not condensed. Only 31% zygotes showed PI-positive stain at 48 h after treatment. TUNEL assay did not reveal DNA fragmentation in pronuclei over 48 h (Table 1). By 72 h after treatment, pronuclei were positively stained with PI, and 46% of zygotes showed weak TUNEL staining. In contrast, intensive treatment of zygotes with 1 mM H_2O_2 for 1.5 h induced shrunken pronuclei and fragmented DNA detected by TUNEL stain as early as 5 h, and more evidently by 24 h after treatment (Fig. 3, C, C′, C″). At 5 h, zygotes underwent degeneration characterized by shrinkage of cytoplasm, membrane permeability to PI, and condensation of pronuclei (Fig. 4). Table 1 shows that cell death occurred in zygotes as early as 5 h after intensive oxidative stress (1 mM H_2O_2 for 1.5 h), while obvious cell death did not occur until 48 h later in zygotes exposed to mild oxidative stress (200 μM H_2O_2 for 15 min). Moreover, the disruption of development and induction of cell death resulted from H_2O_2 itself because catalase, a decomposer of H_2O_2, could completely reverse this effect (data not shown).

Cytochrome c Release and Caspase Activation

We further sought to determine whether cell death of zygotes induced by mild and intense oxidative stress differed in critical biochemical hallmarks, including cytochrome c release and caspase activation. Experiments were replicated three times, with at least 50 embryos observed in each treatment. H_2O_2 treatment of 200 μM for 15 min or 1 mM for 1.5 h induced different dynamics of cytochrome c release and caspase activation. Immunostaining showed that normal zygotes displayed reticulate and punctate staining for cytochrome c (Fig. 5B), coincident with localization of mitochondria ([45, 46], unpublished results). Zygotes treated with 1 mM H_2O_2 for 1.5 h almost invariably exhibited a diffuse distribution of cytochrome c staining, indicative of its release from mitochondria, from 1, 2, 4, and 6 h after treatment until the end of the observation period at 24 h (Fig. 5A). Treatment with 200 μM H_2O_2 for 15 min did not induce cytochrome c release until 72 h after treatment, when clumps of mitochondria and some degree of homogenous cytochrome c distribution appeared in the cytoplasm. Prior to 48 h, there were no detectable changes in cytochrome c localization, although some clumping of mitochondria was noted by JC-1 staining and by ultrastructural observation, as shown below.

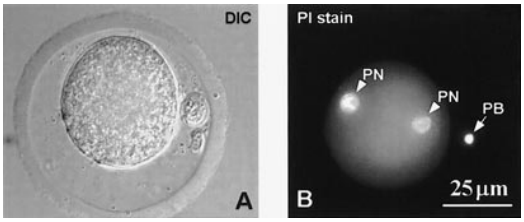

FIG. 4. Zygotes at 5 h after treatment with 1 mM H_2O_2 for 1.5 h displayed cell shrinkage (**A**) and membrane permeability to PI (**B**). PN, Pronucleus; PB, polar body.

Similarly, 200 μM H_2O_2 did not induce caspase activation in zygotes within 48 h after treatment. However, 1 mM H_2O_2 triggered caspase activation as early as 3 h, and active caspase was detected over 24 h. In control, untreated zygotes, low caspase activity was characterized by light yellow-brownish staining, shown in a homogeneous gray appearance (Fig. 6A). The brown or dark brown stain of cytoplasm (early stage) or pronuclei (late stage) indicated active caspase after apoptotic treatment, shown in black in Figure 6, B and C. Similarly, active caspase in the cytoplasm and later in the nuclei was detected in apoptotic oocytes by fluorescence analysis [30]. Treatment with 1 mM H_2O_2 also has been demonstrated to induce activation of caspase 3-like protease in PC 12 cells [41]. Figure 6D shows active caspase stain in blastocysts as a positive control. Indeed, expression of caspase was detected in blastocysts [32, 51]. The active caspase seemed to be correlated with DNA fragmentation in blastocysts.

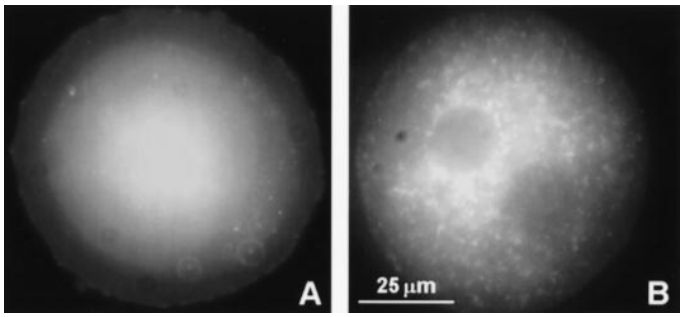

FIG. 5. Fluorescence micrograph showing homogenous distribution of cytochrome c staining, indicating cytochrome c release in zygotes treated with 1 mM H_2O_2 for 1.5 h (**A**), and punctuate localization of cytochrome c in mitochondria in control zygotes (**B**).

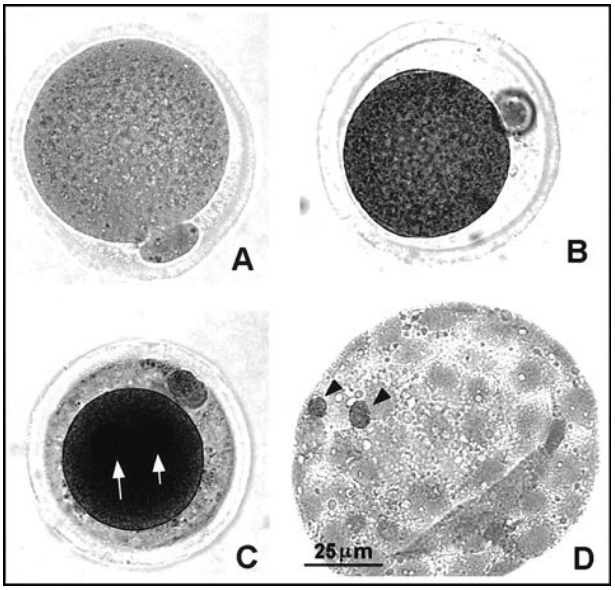

FIG. 6. Caspase activity assay. **A**) Normal zygotes with only slight background staining, indicating absence of caspase activation. **B** and **C**) Brown staining suggestion of active caspase in 1 mM H_2O_2-treated zygotes; very dark brown staining in pronuclei, indicated by two arrows. **D**) Control staining in a blastocyst (two arrowheads indicate active caspase stain in two cells).

Changes in MMP and Distribution of Active Mitochondria

Mild oxidative stress-induced zygotic death appeared more interesting because the prolonged cell cycle arrest mimics cell death of senescent human eggs and because aging is associated with mild oxidation, rather than acute intense stress. We sought to determine whether MMP, distribution, and structure also were affected by mild H_2O_2 treatment, as has been reported in PCD in many somatic cell types. Changes in MMP, assessed by the shift in fluorescence emission and intensity of the dye JC-1, were compared between control untreated zygotes and zygotes treated with 200 μM H_2O_2 1, 2, 3, 4, and 6 h after treatment. In control, normal zygotes preloaded with JC-1, mitochondrial populations with high energy were distributed evenly throughout the cytoplasm, appearing as red fluorescence (Fig. 7, A and B). Living zygotes, like other cells, exhibit both depolarized and hyperpolarized mitochondria [13, 48]. After exposure to 200 μM H_2O_2 for 15 min, the MMP depolarized rapidly, as shown by the dominant green fluorescence in the intermediate region of the cytoplasm, as well as disappearance of red fluorescence and appearance of orange aggregates around cortical regions. Beginning at 2 h after treatment, the pixel ratio intensity, which reflects the MMP, was lower in the intermediate region of H_2O_2-treated embryos than in that of control embryos (Fig. 7C). Perinuclear distribution of active mitochondria was observed in control zygotes, but not in H_2O_2-treated zygotes (Fig. 8).

Ultrastructural Observation of Mitochondria

In untreated, control zygotes (Fig. 9), the sphere-shaped, vacuolated, immature mitochondria exhibited electron-dense matrices without obvious cristae. Mitochondria were scattered throughout the intermediate region of the cytoplasm (Fig. 9, upper panels). In zygotes treated with 200 μM H_2O_2, alterations of mitochondrial structure, including

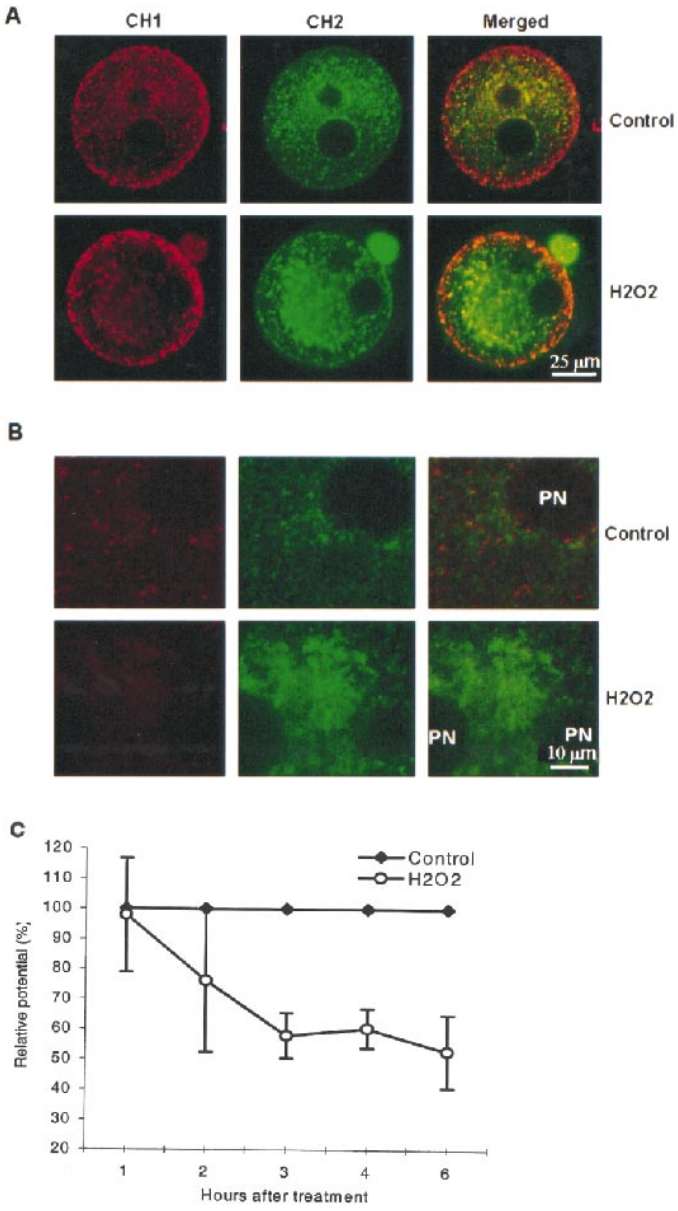

FIG. 7. Confocal microscopy imaging of mitochondria in mouse zygotes stained with JC-1. **A**) Channel 1 with red (hyperpolarized, J aggregates), channel 2 with green (monomer form of JC-1), and merged fluorescence (for ratio image analysis) in control cultured zygotes and 200 μM H_2O_2-treated zygotes at 4 h. **B**) Higher magnification in the central cytoplasm of zygotes. PN, Pronucleus. **C**) The ratio imaging analysis collected from the confocal images. The average of relative MMP from control zygotes at each time point was set at 100%, and the MMP in treated zygotes were expressed relative to control for that time point. MMP in zygotes declined from 2 h after treatment of 200 μM H_2O_2 for 15 min and continued to drop over the subsequent hours. Data are presented as means ± SD in three replicates.

disruption of the matrix, were noted at 2 h. By 4 h after treatment, further loss of matrix and increased vacuole size were found (Fig. 9, B and D). It appeared that the membrane was damaged in some mitochondria. Furthermore, mitochondria aggregated within the cytoplasm (Fig. 9, upper panel). We did not see obvious structural changes in other organelles, including nuclear envelope and nucleoli.

DISCUSSION

Our data demonstrate that H_2O_2 induces cell cycle arrest and cellular changes consistent with PCD in mouse zygotes

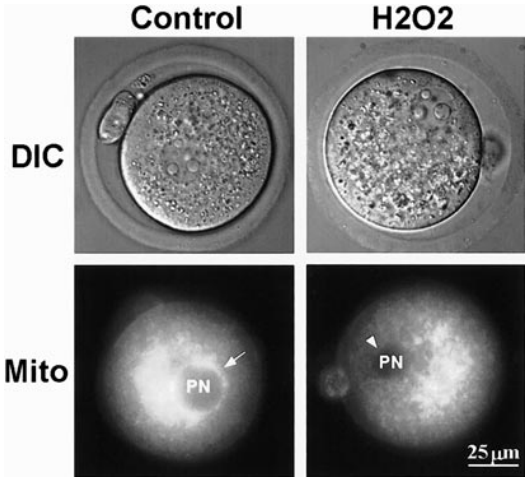

FIG. 8. MitoTracker staining of active mitochondria in zygotes. Perinuclear distribution of mitochondria was seen (arrow) in control zygotes but absent (arrowhead) around the pronuclei (PN) in zygotes treated with 200 μM H_2O_2. Under differential interference contrast imaging, the pronuclei could be seen intact in both group zygotes. Different embryos were visualized under differential interference contrast and fluorescence.

and that mitochondria are involved in these oxidative stress-induced processes.

Oxidative Stress-Induced Zygotic Cell Cycle Arrest, Apoptosis, and/or Necrosis?

Mild oxidation treatment of zygotes initially led to decline in MMP, alteration of mitochondrial matrix, and change in the cellular distribution of mitochondria. Morphologically, the zygotes shrank but did not show the typical biochemical hallmarks of PCD, such as cytochrome c release, caspase activation, and DNA fragmentation (TUNEL-positive stain) during the first 48 h after treatment. Rather, only after 72 h of developmental arrest did they exhibit nuclear DNA fragmentation. Extensive evidence has documented that H_2O_2 induces apoptosis in a variety of cell systems and also acts as a second messenger during apoptotic signal transduction [7, 8, 52, 53]. The discovery that the anti-apoptotic Bcl-2 gene product has antioxidant properties further supports the importance of oxidative events in apoptosis [8, 9]. We propose that mitochondrial dysfunction may contribute to both cell cycle arrest and apoptosis during early embryo development. In fact, cell cycle arrest and apoptosis may be interconnected, and the G1→S transition of the cell cycle is the most susceptible point for cells to implement a death program [54]. Although we did not determine the specific stage of cell cycle arrest in this experiment, mitotic phase was not observed in zygotes even 72 h after H_2O_2 treatment.

H_2O_2 has been shown to induce either apoptosis or features of senescence, depending on the concentration employed or the cell lines treated. Higher concentrations of H_2O_2 increase the proportion of cells undergoing apoptosis [55]. Before the induction of apoptosis, many cells enter a transient phase of cell cycle arrest. Low levels of H_2O_2 induce many features of senescence in vitro, including cell cycle arrest, inhibition of DNA synthesis, and induction of single-strand breaks in DNA [36, 55–57]. In several mammalian cell lines, H_2O_2 at concentrations between 150 and 300 μM inhibit cell division, whereas high concentrations of H_2O_2 (≥ 1 mM) induce cell death with features of both apoptosis and necrosis [58]. The present experiments with

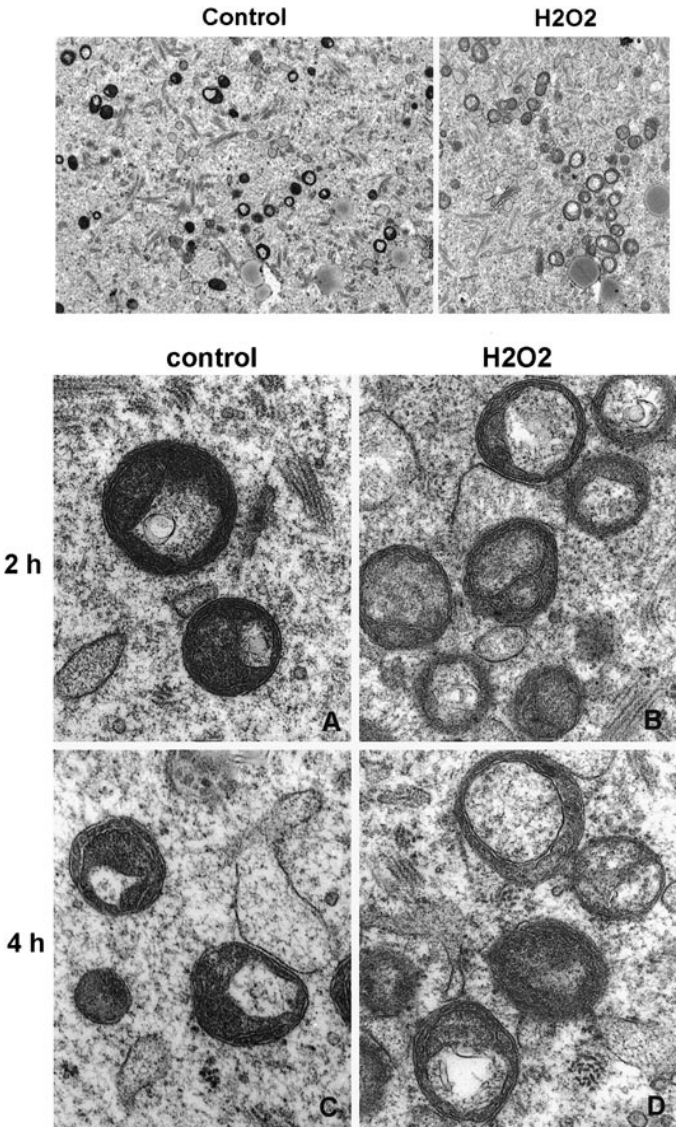

FIG. 9. Electron micrographs of mitochondrial ultrastructure of mouse zygotes treated with 200 μM H_2O_2. Top: Mitochondrial homogenous distribution in the intermediate region of control zygotes and aggregation of mitochondria in the cytoplasm in H_2O_2-treated zygotes. ×4000. **A, C**) Control zygotes; **B, D**) H_2O_2-treated zygotes showing alteration of mitochondria ultrastructure in matrix or membrane. ×34 000.

mouse zygotes demonstrated similar dose-dependent effects of H_2O_2 on cell death in zygotes.

Treatment of mouse zygotes with high-dose H_2O_2 led to early cell shrinkage, membrane blebbing, and pronuclear condensation, consistent with the classical morphological definition of apoptosis [18, 19]. Moreover, shortly after treatment, cytochrome c was released and caspase was activated, followed by DNA fragmentation in pronuclei. Intensive oxidation also might result in necrosis in zygotes as shown by their permeability to PI stain, indicative of membrane disruption. Nevertheless, swollen cells, the typical morphological change of necrosis, never were observed after intensive oxidative treatment of zygotes. Instead, shrinkage of cells appeared consistently. During necrosis, the loss of oxidative phosphorylation leads to loss of mitochondrial volume homeostasis and acute depletion of mitochondrial-derived ATP [59]. ATP is required for the orchestrated destruction of the cell that characterizes apoptosis, including cytochrome c-induced caspase activation

[60]. The cytochrome c release and caspase activation observed in H_2O_2-treated zygotes suggests that ATP was available at least for the initial phase. Presumably as intracellular ATP is depleted, cell death shifts from an apoptotic to a necrotic form of cell death [61]. More evidence suggests that the two forms of cell death share similar signaling pathway and execution events, and that the necrosis may not be a passive response to extensive damage, as demonstrated by H_2O_2 treatment of some somatic cells [62–65].

Together, depending on concentration and/or exposure time, H_2O_2 may induce cell cycle arrest, apoptosis, or necrosis in early mammalian embryos. Intensive treatment with H_2O_2 induced PCD, while mild treatment induced cell cycle arrest followed by delayed PCD. Interestingly, the cell cycle arrest and apoptosis observed after mild H_2O_2 treatment mimics the behavior of apoptotic embryos from older women. At present, it is unclear whether the pharmacologically induced cellular events we described here underlie the decreased developmental potential of fertilized oocytes from older infertile women. It might be possible that some apoptotic machinery in the oxidative model participate in determining embryo viability.

Mitochondrial Involvement in Cell Death in Zygotes

Mitochondria play a crucial role in the early stages of apoptosis. In many systems, the release of pro-apoptotic factors, such as cytochrome c or apoptosis-inducing factor, from the mitochondrial intermembrane space into the cytosol has been demonstrated to be a primary event in caspase activation and nuclear apoptosis [14, 44, 60, 66–68]. Both the loss of outer mitochondrial membrane integrity, leading to cytochrome c release, and inner membrane depolarization are caspase-activating agents that trigger the apoptotic cascade downstream of Bcl-XL [63].

The present study showed that intensive H_2O_2 treatment induced cytochrome c release and activation of caspase-3, followed by nuclear DNA fragmentation, with a time course suggesting that cytochrome c release is an early event in apoptosis in the mouse zygote. Recently, caspase activity in mouse zygotes also was detected after treatment with staurosporine [51]. Cytochrome c release and caspase activation also have been observed in H_2O_2-induced apoptosis in somatic cells [69]. Western blot assay has been extensively used for detection of cytochrome c localization in cytosol versus mitochondria. Yet there is no reliable method available to separate mitochondria from cytosol in zygotes. By using immunocytochemistry [45, 46], we directly observed cytochrome c release from mitochondria in mouse zygotes. These data in mammalian embryos provide further evidence to confirm the importance of early cytochrome c release from mitochondria in the PCD in early embryos, even though mitochondria are relatively immature.

Disruption of the outer mitochondrial membrane could precede the loss of MMP [47]. Mitochondrial cytochrome c release could occur in the absence of mitochondrial depolarization, and collapse of the inner mitochondrial transmembrane potential might not be required for apoptosis in some types of cells [66, 67, 69, 70]. Cytochrome c may exit mitochondria via a different route, e.g., the voltage-dependent anion channel [71], than the mitochondrial permeability transition pore (MPT). Thus, in certain systems, cytochrome c release and apoptosis could be independent of the permeability transition pore [45]. Oxidative stress can change MMP and MPT ([11, 72], present study with mild oxidative stress). Whether MPT is the main pathway involved in the oxidative stress-induced cell death in the zygote needs further investigation.

On the ultrastructural level, zygote mitochondria appear as small, vacuolated, electron-dense matrix structures as observed previously [23]. These fine structures are associated with the low oxygen consumption and ATP production [24]. After oxidative stress by mild H_2O_2 treatment, mitochondria aggregated in the cytoplasm, and the matrix and/or membrane was disrupted. Moreover, we also observed a shift in distribution of active mitochondria after H_2O_2 treatment, i.e., a lack of perinuclear clustering of active mitochondria, consistent with malfunction of mitochondria, which may result in the failure in mitotic entry.

To summarize, both mild and intensive oxidative stress induced cell death of zygotes. Mild oxidative stress induced cell cycle arrest, followed by delayed apoptotic cell death, possibly through altering mitochondrial activity and structures; intensive oxidative stress probably triggered apoptosis and terminal necrosis through early cytochrome c release from mitochondria and caspase activation. Therefore, the present study provides evidence that mitochondria are involved in the oxidative stress-induced cell cycle arrest and cell death in a single cell system, mammalian zygotes.

ACKNOWLEDGMENTS

The authors wish to thank Dr. Peter Smith for his valuable discussion and encouragement and Mr. Louis Kerr for his enthusiastic assistance with electronic microscopy.

REFERENCES

1. Johnson FB, Sinclair DA, Guarente L. Molecular biology of aging. Cell 1999; 96:291–302.
2. Ozawa T. Genetic and functional changes in mitochondria associated with aging. Physiol Rev 1997; 77:425–464.
3. Papa S, Skulachev VP. Reactive oxygen species, mitochondria, apoptosis and aging. Mol Cell Biochem 1997; 174:305–319.
4. Shigenaga MK, Hagen TM, Ames N. Oxidative damage and mitochondrial decay in aging. Proc Natl Acad Sci USA 1994; 91:10771–10778.
5. Sohal RS, Weindruch R. Oxidative stress, caloric restriction, and aging. Science 1996; 273:59–63.
6. Wei YH. Oxidative stress and mitochondrial DNA mutations in human aging. Proc Soc Exp Biol Med 1998; 217:53–63.
7. Buttke TM, Sandstrom PA. Oxidative stress as mediator of apoptosis. Immunol Today 1994; 15:7–10.
8. Hockenbery DM, Oltvai ZN, Yin XM, Milliman CL, Korsmeyer SJ. Bcl-2 functions in an antioxidant pathway to prevent apoptosis. Cell 1993; 75:241–251.
9. Kane DJ, Sarafian TA, Anton R, Hahn H, Gralla FB, Valentine JS, Ord T, Bredesen DE. Bcl-2 inhibition of neural death: decreased generation of reactive oxygen species. Science 1993; 262:1274–1277.
10. Quillet-Mary A, Jaffrezou JP, Mansat V, Bordier C, Naval J, Laurent G. Implication of mitochondrial hydrogen peroxide generation in ceramide-induced apoptosis. J Biol Chem 1997; 272:21388–21395.
11. Kowaltowski AJ, Vercesi AE. Mitochondrial damage induced by conditions of oxidative stress. Free Radical Biol Med 1999; 26:463–471.
12. Cai J, Yang J, Jones DP. Mitochondrial control of apoptosis: the role of cytochrome c. Biochim Biophys Acta 1998; 1366:139–149.
13. Petit PX, Lecoeur H, Zorn E, Dauguet C, Mignotte B, Gougeon ML. Alterations in mitochondrial structure and function are early events of dexamethasone-induced thymocyte apoptosis. J Cell Biol 1995; 130: 157–167.
14. Kroemer G, Zamzami N, Susin SA. Mitochondrial control of apoptosis. Immunol Today 1997; 18:44–51.
15. Mignotte B, Vayssiere JL. Mitochondria and apoptosis. Eur J Biochem 1998; 252:1–15.
16. Slater AFG, Stefan C, Nobel I, van den Dobblesteen DJ, Orrenius S. Intracellular redox changes during apoptosis. Cell Death Differ 1996; 3:57–62.

17. Wyllie AH, Kerr JFR, Currie AR. Cell death: the significance of apoptosis. Int Rev Cytol 1980; 68:251–306.
18. Warner CM, Exley GE, McElhinny AS, Tang C. Genetic regulation of preimplantation mouse embryo survival. J Exp Zool 1998; 282: 272–279.
19. Harmon BV, Winterford CM, O'Brien BA, Allan DJ. Morphological criteria for identifying apoptosis. In: Celis JE (ed.), Cell Biology: A Laboratory Handbook (second edition), Vol. 1. San Diego: Academic Press; 1998: 327–339.
20. Bonfoco E, Krainc D, Ankarcrona M, Nicotera P, Lipton SA. Apoptosis and necrosis: two distinct events induced respectively by mild and intense insults with *N*-methyl-D-aspartate or nitric oxide/superoxide in cortical cell cultures. Proc Natl Acad Sci USA 1995; 92: 7162–7166.
21. Leist MF, Gantner F, Bohlinger I, Germann PG, Tiegs G, Wendel A. TNF-induced murine hepatic apoptosis as a pathomechanism of septic liver failure. Am J Pathol 1995; 166:1–15.
22. Green DR, Reed JC. Mitochondria and apoptosis. Science 1998; 281: 1309–1312.
23. Stern S, Biggers JD, Anderson E. Mitochondria and early development of the mouse. J Exp Zool 1971; 176:179–192.
24. Biggers JD, Borland RM. Physiological aspects of growth and development of the preimplantation mammalian embryos. Annu Rev Physiol 1976; 38:95–119.
25. Houghton FD, Thompson JG, Kennedy CJ, Leese HJ. Oxygen consumption and energy metabolism of the early mouse embryo. Mol Reprod Dev 1996; 44:476–485.
26. Keefe DL. Reproductive aging is an evolutionarily programmed strategy that no longer provides adaptive value. Fertil Steril 1998; 70:204–206.
27. Navot D, Bergh P, Williams MA, Garrisi GJ, Guzman I, Sandler B, Grundfeld L. Poor oocyte quality rather than implantation failure as a cause of age-related decline in female fertility. Lancet 1991; 337: 1375–1377.
28. Janny L, Menezo YJR. Maternal age effect on early human embryonic development and blastocyst formation. Mol Reprod Dev 1996; 45:31–37.
29. Perez GI, Robles R, Knudson CM, Flaws JA, Korsmeyer SJ, Tilly JL. Prolongation of ovarian lifespan into advanced chronological age by Bax-deficiency. Nat Genet 1999; 21:200–203.
30. Perez GI, Tao XJ, Tilly JL. Fragmentation and death (a.k.a. apoptosis) of ovulated oocytes. Mol Human Reprod 1999; 5:414–420.
31. Jurisicova A, Latham KE, Casper RF, Varmuza SL. Expression and regulation of genes associated with cell death during murine preimplantation embryo development. Mol Reprod Dev 1998; 51:243–253.
32. Moley KH, Chi MM, Knudson CM, Korsmeyer SJ, Mueckler MM. Hyperglycemia induces apoptosis in pre-implantation embryos through cell death effector pathways. Nat Med 1998; 4:1421–1424.
33. Pierce GB, Parchment RE, Lewellyn AL. Hydrogen peroxide as a mediator of programmed cell death in the blastocyst. Differentiation 1991; 46:181–186.
34. Yang HW, Hwang KJ, Kwon HC, Kim HS, Choi KW, Oh KS. Detection of reactive oxygen species (ROS) and apoptosis in human fragmented embryos. Hum Reprod 1998; 13:998–1002.
35. Nasr-Esfahani MH, Aitken JR, Johnson MH. Hydrogen peroxide levels in mouse oocytes and early cleavage stage embryos developed in vitro or in vivo. Development 1990; 109:501–507.
36. Gille JJP, Joenje H. Cell culture models for oxidative stress: superoxide and hydrogen peroxide versus normobaric hyperoxia model for aging studies. Mutat Res 1992; 275:405–414.
37. Lawitts JA, Biggers JD. Culture of preimplantation embryos. In: Wassarman PM, DePamphilis ML (eds.), Guide to Techniques in Mouse Development, Methods in Enzymology. San Diego: Academic Press; 1993:153–164.
38. Liu L, Trimarchi JR, Keefe DL. Thiol oxidation-induced embryonic cell death in mice is prevented by the antioxidant dithiothreitol. Biol Reprod 1999; 61:1162–1169.
39. Liu Z, Foote RH. Effects of amino acids on the development of in-vitro matured in-vitro fertilized bovine embryos in a simple protein-free medium. Hum Reprod 1995; 10:2985–2991.
40. Kaal ECA, Veldman H, Sodaar P, Joosten EJA, Bar PR. Oxidant treatment causes a dose-dependent phenotype of apoptosis in cultured motoneurons. J Neurosci Res 1998; 54:778–786.
41. Okuno S, Shimizu S, Ito T, Nomura M, Hamada E, Tsujimoto Y, Matsuda H. Bcl-2 prevents caspase-independent cell death. J Biol Chem 1998; 273:34272–34277.
42. Jacobson MD, Burne JF, Raff MC. Programmed cell death and BCL-2 protection in the absence of a nucleus. EMBO J 1994; 13:1899–1910.
43. Brison DR, Schultz RM. Apoptosis during mouse blastocyst formation: evidence for a role for survival factors including transforming growth factor α. Biol Reprod 1997; 56:1088–1096.
44. Yoshida H, Kong YY, Yoshida R, Elia AJ, Hakem A, Hakem R, Penninger JM, Mak TW. Apaf1 is required for mitochondrial pathways of apoptosis and brain development. Cell 1998; 94:739–750.
45. Eskes R, Antonsson B, Osen-Sand A, Montessuit S, Richter C, Sadoul R, Mazzei G, Nichols A, Martinou JC. Bax-induced cytochrome C release from mitochondria is independent of the permeability transition pore but highly dependent on Mg^{2+} ions. J Cell Biol 1998; 143: 217–224.
46. Desagher A, Osen-Sand A, Nichols A, Eskes R, Montessuit S, Lauper S, Maundrell K, Antonsson B, Martinou JC. Bid-induced conformational change of Bax is responsible for mitochondrial cytochrome c release during apoptosis. J Cell Biol 1999; 144:891–901.
47. Smiley ST, Reers M, Mottola-Hartshorn C, Lin M, Chen A, Smith TW, Steele GD Jr, Chen LB. Intracellular heterogeneity in mitochondrial membrane potentials revealed a J-aggregate-forming lipophilic cation JC-1. Proc Natl Acad Sci USA 1991; 88:3671–3675.
48. Reers M, Smiley ST, Mottola-Hartshorn C, Chen A, Lin M, Chen LB. Mitochondrial membrane potential monitored by JC-1 dye. Methods Enzymol 1995; 260:406–417.
49. Barnett DK, Kimura J, Bavister BD. Translocation of active mitochondria during hamster preimplantation embryo development studied by confocal laser scanning microscopy. Dev Dyn 1996; 205:64–72.
50. Weil M, Jacobson MD, Coles HSR, Davies TJ, Gardner RL, Raff KD, Raff MC. Constitutive expression of the machinery for programmed cell death. J Cell Biol 1996; 133:1053–1059.
51. Exley GE, Tang C, McElhinny AS, Warner CM. Expression of caspase and Bcl-2 apoptotic family membrane in mouse preimplantation embryos. Biol Reprod 1999; 61:231–239.
52. Forrest VJ, Kang YH, McClain DE, Robinson DH, Ramakrishnan N. Oxidative stress-induced apoptosis prevented by trolox. Free Radical Biol Med 1994; 16:675–684.
53. Tada-Oikawa S, Oikawa S, Kawanishi M, Yamada M, Kawanishi S. Generation of hydrogen peroxide precedes loss of mitochondrial membrane potential during DNA alkylation-induced apoptosis. FEBS Lett 1999; 442:65–69.
54. Meikrantz W, Schlegel R. Apoptosis and the cell cycle. J Cell Biochem 1995; 58:160–174.
55. Bladier C, Wolvetang EJ, Hutchinson P, de Hann JB, Kola I. Response of a primary human fibroblast cell line to H_2O_2: senescence-like growth arrest or apoptosis? Cell Growth Differ 1997; 8:589–598.
56. Chen Q, Ames BN. Senescence-like growth arrest induced by hydrogen peroxide in human diploid fibroblast F65 cells. Proc Natl Acad Sci USA 1994; 91:4130–4134.
57. Clopton DA, Saltman P. Low-level oxidative stress causes cell-cycle specific arrest in cultured cells. Biochem Biophys Res Commun 1995; 210:189–196.
58. Wiese AG, Pacifici RE, Davies KJA. Transient adaptation to oxidative stress in mammalian cells. Arch Biochem Biophys 1995; 318:231–240.
59. Lemasters JJ, DiGuiseppi J, Nieminen AL, Herman B. Blebbing, free Ca^{2+} and mitochondrial membrane potential preceding cell death in hepatocytes. Nature 1987; 325:78–81.
60. Liu X, Kim CN, Yang J, Jemmerson R, Wang X. Induction of apoptotic program in cell-free extracts: requirement for dATP and cytochrome c. Cell 1996; 86:147–157.
61. Eguchi Y, Shimizu S, Tsujimoto Y. Intracellular ATP levels determine cell death fate by apoptosis or necrosis. Cancer Res 1997; 57:1835–1840.
62. Warny M, Kelly C. Monocyte cell necrosis is mediated by potassium depletion and caspase-like proteases. Am J Physiol 1999; 276:C717–724.
63. Vander Heiden MG, Chandel NS, Williamson EK, Schumacker PT, Thompson CB. Bcl-X_l regulates the membrane potential and volume homeostasis of mitochondria. Cell 1997; 91:627–637.
64. Leist M, Nicotera P. The shape of cell death. Biochem Biophys Res Commun 1997; 236:1–9.
65. Xu Y, Bradham C, Brenner DA, Czaja MJ. Hydrogen peroxide-induced liver cell necrosis is dependent on AP-1 activation. Am J Physiol 1997; 273:G795–803.
66. Yang J, Liu X, Bhalla K, Kim CN, Ibrado AM, Cai J, Peng TI, Jones

DP, Wang X. Prevention of apoptosis by Bcl-2: release of cytochrome c from mitochondria blocked. Science 1997; 275:1129–1132.
67. Kluck RM, Bossy-Wetzel E, Green DR, Newmeyer DD. The release of cytochrome c from mitochondria: a primary site for Bcl-2 regulation of apoptosis. Science 1997; 275:1132–1136.
68. Susin SA, Lorenzo HK, Zamami N, Marzo I, Snow BE, Brothers GM. Molecular characterization of mitochondrial apoptosis-inducing factor. Nature 1999; 397:441–446.
69. Stridh H, Kimland M, Jones DP, Orrenius S, Hampton MB. Cytochrome c release and caspase activation in hydrogen peroxide- and tributyltin-induced apoptosis. FEBS Lett 1998; 429:351–355.
70. Finucane DM, Waterhouse NJ, Amarante-Mendes GP, Cotter TG, Green DR. Collapse of the inner mitochondrial transmembrane potential is not required for apoptosis of HL60 cells. Exp Cell Res 1999; 251:166–174.
71. Shimizu S, Narita M, Tsujimoto Y. Bcl-2 family proteins regulate the release of apoptogenic cytochrome c by the mitochondrial channel VDAC. Nature 1999; 399:483–487.
72. Robb SJ, Robb-Gaspers LD, Scaduto RC Jr, Thomas AP, Connor JR. Influence of calcium and iron on cell death and mitochondrial function in oxidatively stressed astrocytes. J Neurosci Res 1999; 55:674–686.